XMM-Newton CCF Release Note

XMM-CAL-SRN-0312

RDPHA calibration in the Fe line regime for EPIC-pn Timing Mode

Matteo Guainazzi

28 February 2014

1 CCF components

Name of CCF	VALDATE	EVALDATE	Blocks changed	XSCS flag
EPN_CTI_0032.CCF	2000-01-01T00:00:00		RDPHA_DERIV[a]	NO
EPN_CTI_0033.CCF	2012-07-01T20:11:48		RDPHA_DERIV[a]	NO

[a]the `RDPHA_DERIV` extensions in these CCF constituents is the same. However, their `LONG_TERM_CTI` extensions differ (Smith et al., 2014). These extensions apply to different time intervals, as specified by the latter `VALDATE` keyword.

The "Rate-Dependent PHA" (RDPHA) correction was introduced with SASv13 as an alternative (and, prospectively, more robust) method to correct for count-rate dependent effects on the energy scale of EPIC-pn exposures in Timing Mode (Guainazzi, 2013a). With SASv13.5, a tabular calibration as a function of the rate of shifted electron domain was introduced, replacing the original imperfect linear calibration (Guainazzi, 2013b). The RDPHA is intended to ultimately supersede the Rate-Dependent CTI (RDCTI) correction (Guainazzi et al., 2008), whose energy-dependence is based on unverified (and probably inaccurate) assumptions (Guainazzi & Smith 2013).

We describe in this Release Note (RN) the calibration of the RDPHA at the energies of iron atomic transitions ($\simeq$6.4–7 keV). This is the first *direct calibration of the hard X-ray energy scale in EPIC-pn Timing Mode exposures*. It has been made possible by the combination of an improved understanding of the instrument performances in this Mode, and of the availability of sufficient data at a count rate level close to the pile-up threshold ($\simeq$800 s^{-1}; Guainazzi et al., 2013b).

2 Changes

I analysed the spectra of four sources, exhibiting strong narrow-band absorption and emission line features due to highly ionised (H- and He-like) iron (Tab. 1). and observed after

Table 1: List of XMM-Newton observations used for the high-energy calibration of the RDPHA

Source	Obs.#	Iron lines	Reference
XB 1323-619	0036140201	FeXXVK$_\alpha$, FeXXVIK$_\alpha$ (abs.)	Boirin et al. 2005
4U1915-05	0085290301	FeXXVK$_\alpha$, FeXXVIK$_\alpha$, K$_\beta$ (abs.)	Boirin et al., 2004
RS Oph	0410180101	FeXXVK$_\alpha$ (emi.)	Ness et al., 2007
GX13+1	0505480101	FeXXVK$_\alpha$, K$_\beta$, FeXXVIK$_\alpha$, K$_\beta$ (abs.)	Díaz-Trigo et al., 2012

the 7^{th} of July 2002[1] Calibrated event lists were produced using the reduction meta-task `epchain` with standard parameters. In particular, I applied the X-Ray Loading (XRL) correction as recommended as of SASv13.5 (Guainazzi & Smith 2013). For each EPIC-pn exposure I extracted spectra from the four columns around the boresight. Background spectra were extracted from a 4 columns-wide box close to the CCD edge (`RAWX` = 2-6). Responses were generated for each source spectrum using the SAS tasks `arfgen` and `rmfgen`. Spectra were rebinned to have at least 100 background-subtracted counts in each spectral channel, and not to oversample the instrumental resolution by a factor >3 to ensure the applicability of the χ^2 goodness-of-fit test. I applied an energy-independent systematic error of 1% on the effective area calibration[2] through the command `systematic` in XSPEC (used for the spectral analysis). I fit the spectra in the 3–10 keV energy band to avoid spectral complexity not directly related to the estimate of the energy scale in the hard band. Models were extracted from the references listed in Tab. 1. An astrophysical interpretation of the spectral components used to model the spectra discussed hereafter is beyond the scope of this RN.

In order to estimate the deviations from the correct energy scale, I assumed in the spectral fitting that the narrow-band features listed in Tab. 1 are at their nominal laboratory energy. I measured the corresponding global change in the energy scale through the command `gain fit` in XSPEC[3]. I applied astrophysical offsets to the spectral models of RS Oph and GX13+1 following the analysis of Ness et al. (2007) and Díaz-Trigo et al. (2012), respectively, although in the latter case I have assumed a smaller outflow velocity as published by them (corresponding to a blue-shift of 0.002; Maria Díaz-Trigo, private communication)

The results are shown in Fig. 1. The global energy shifts (ΔE) are plotted as a function of the average rate of shifted electron, N_e during the observation, the relevant parameter for the estimate of rate-dependent effects on the energy scale (Guainazzi et al., 2008). While many data points are affected by large statistical uncertainties, a general increasing trend of the energy scale discrepancy with count rate exists. I fit the data with a Gompertz function:

$$\Delta E = (84 \pm 3) \times e^{(-7\pm3)\times e^{-(0.0033\pm0.006)N_e}}$$

[1]ODFs of EPIC-pn exposures taken before that date do not contain a dumped offset map. Consequently the XRL correction in EPIC-pn Timing Mode exposures is not entirely reliable (Smith 2004).

[2]This number is the outcome of a still unpublished study on the systematic uncertainties of the EPIC-pn effective area above 2 keV. Once completed, this study will be published in the EPIC Calibration Status Document, available at: `http://xmm2.esac.esa.int/docs/documents/CAL-TN-0018.pdf`.

[3]In principle this approach is not rigorous, because `gain fit` shifts the energy scale of the response rather than that of the spectrum. However, it has been proven that the two approaches yield consistent results (Marinucci et al., submitted.)

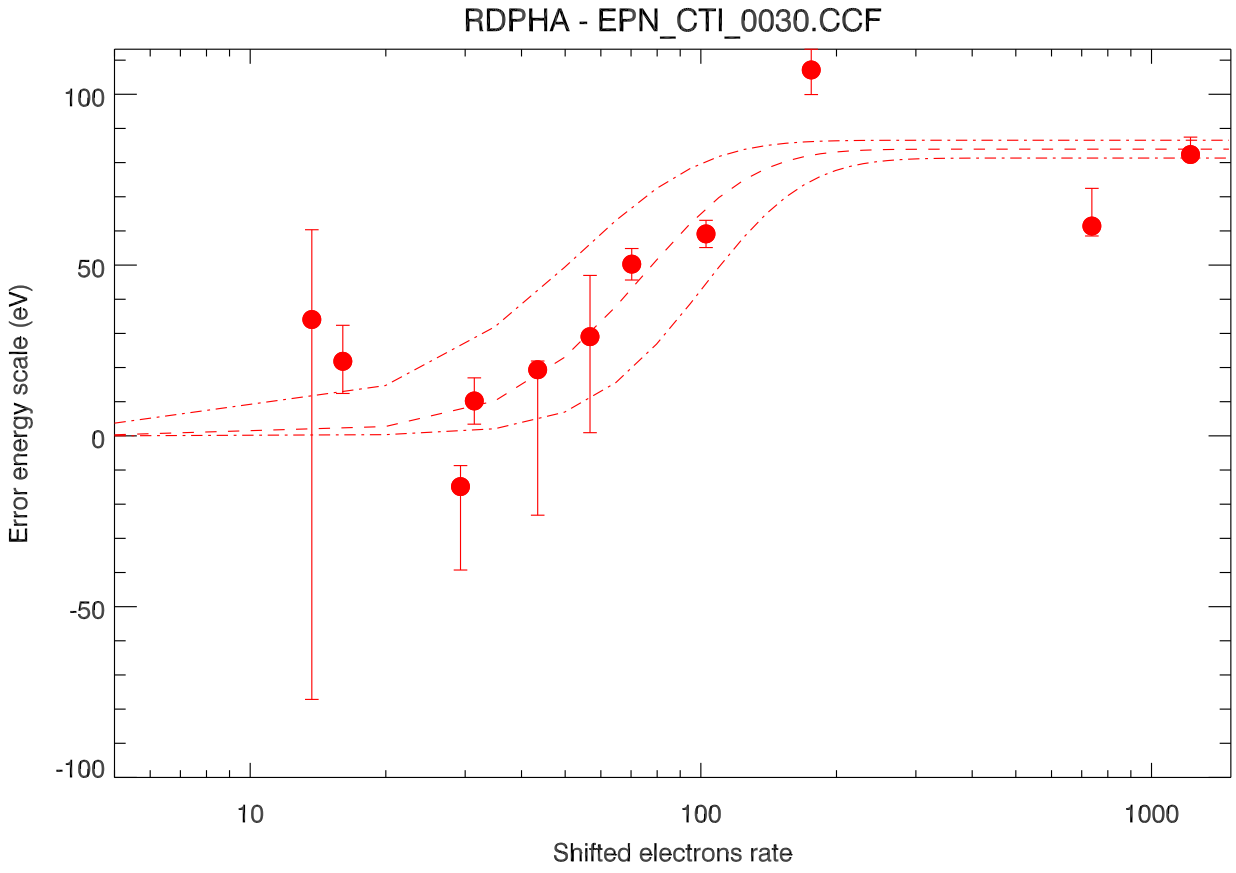

Figure 1: Deviation from the nominal energy scale in the Fe energy band as a function of the average rate of shifted electrons for the observations in Tab. 1. The *dashed line* is the best-fit with a Gompertz function; the *dashed-dotted* lines indicate the envelope of the 1σ error on the best-fit parameters.

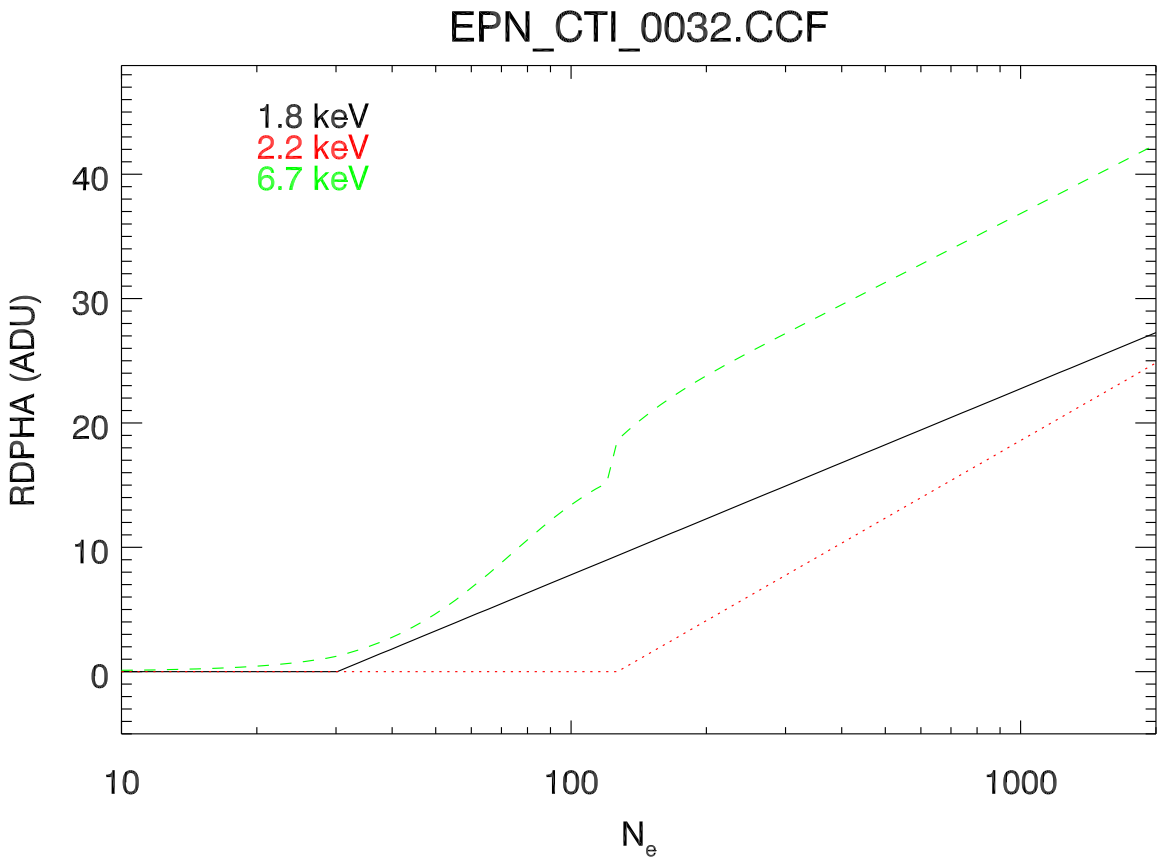

Figure 2: RDPHA correction in `EPN_CTI_0032.CCF`. The energies in the *inset* refer to the nominal energy to which the RDPHA correction is applied. A linear interpolation is used by `epevents` to correct the PHA scale of events at intermediate values.

Errors on the best-fit parameters are quoted at the 1σ level.

3 Scientific Impact of this Update

We used the calibration of the ΔE versus N_e function in Sect. 2 to modify the RDPHA correction function (Guainazzi 2013b). The current calibration functions are shown in Fig. 2.

4 Estimated Scientific Quality

The goal of this update is bringing the accuracy of the energy scale in EPIC-pn Timing Mode exposures in the iron regime (*i.e.*: $\simeq$6.4–7 keV) to the same level already achieved at the energies of the instrumental edges ($\simeq$1.8–2.2 keV): $\pm$20 eV (1σ; Guainazzi 2013b).

Table 2: Post-RDPHA accuracy (ΔE_{RDPHA}) of the energy scale at the Fe line energies.

Source	Obs.#	N_e	ΔE_{RDPHA} (eV)
4U1915-05	0085290301	11.1	-13 ± 20
RS Oph	0410180101	20.6	6 ± 2
GX13+1	0505480101	241.2	16 ± 5
GX13+1	0505480301	245.9	$22 \pm^{6}_{8}$
GX13+1	0505480401	223.8	$18 \pm^{2}_{8}$
GX13+1	0505480501	226.9	-14 ± 1

5 Test procedures and results

I tested the accuracy of the energy scale achieved with this update of the RDPHA by analysing spectra extracted from event lists on which the `EPN_CTI_0032.CCF` constituent had been applied. I selected a sub-set of the sources in Tab. 1, covering the range in N_e between $\simeq$10 to $\simeq$300. It goes without saying that this does not represent a full independent validation of the RDPHA performances in the hard energy band, because there is a significant overlap between the calibration and the validation data-sets. Unfortunately, this exercise is primarily limited by the lack of X-ray spectra, where reliable narrow-band absorption or emission features can be identified and measured. In order to extend the sample of validation sources, I analysed all the available spectra of GX13+1 in the science archive. Source spectra were extracted from internals of $\pm$9 pixels in `RAWX` around the boresight column. Otherwise, the data reduction and analysis followed the same procedure as described in Sect. 2.

In all cases the post-RDPHA accuracy of the energy scale is consistent with being better then $\pm$20 eV (Tab. 2). However, we urge users to exercise caution in interpreting these results. As shown in Fig. 1, the high-energy calibration of the RDPHA is based on just a handful of sources, exhibiting appropriate spectral features (as opposed to the RDPHA calibration at the instrumental edges, that employed several dozens of sources; Guainazzi 2013b). The calibration dataset inevitably covers only a comparatively small range in count rate and hardness ratio. Users are warmly recommended to exercise astrophysical common sense in interpreting results obtained in the high-energy band with EPIC-pn Timing Mode exposures, if accuracies of the energy scale better than 50 eV are crucial for their science.

6 Expected updates

With this update, the recalibration of the energy scale of EPIC-pn Timing Mode following the discovery of ubiquitous XRL (Guainazzi & Smith, 2013) is completed. A systematic of $\pm$20 eV has to be considered the unavoidable limit to the nominal accuracy of the energy scale in this mode, due to its readout pattern. No further improvements are foreseen.

Acknowledgments

The work underlying the RN would have not been possible without the continuous support, advise, and patient encouragement by several members of the XMM-Newton astronomical community. Special acknowledgements are due to: Tiziana Di Salvo, Maria Díaz-Trigo, Chris Done, Mari Kolehmainen, and Mariano Mendez.

7 References

Boirin et al., 2004, A&A, 418, 1061

Boirin L., et al., 2005, A&A, 436, 195

Díaz-Trigo et al., 2012, A&A, 543, 50

Guainazzi M., 2013a, XMM-SOC-CAL-SRN-0299 (available at `http://xmm2.esac.esa.int/docs/documents/CAL-SRN-0299-1-1.ps.gz`)

Guainazzi M., 2013b, XMM-SOC-CAL-SRN-0306 (available at `http://xmm2.esac.esa.int/docs/documents/CAL-SRN-0306-1-1.pdf`)

Guainazzi M. & Smith M., 2013, XMM-SOC-CAL-SRN-0306 (available at `http://xmm2.esac.esa.int/docs/documents/CAL-SRN-0302-1-5.pdf`)

Guainazzi M., et al., 2008, XMM-SOC-CAL-SRN-0248 (available at `http://xmm2.esac.esa.int/docs/documents/CAL-SRN-0248-1-0.ps.gz`)

Guainazzi M., et al., 2013a, XMM-SOC-CAL-TN-0018 (available at `http://xmm2.esac.esa.int/docs/documents/CAL-TN-0018.pdf`)

Guainazzi M., et al., 2013b, XMM-SOC-CAL-TN-0083 (available at `http://xmm2.esac.esa.int/docs/documents/CAL-TN-0083.pdf`)

Ness J.-U., et al., 2007, ApJ, 665, 1334

Smith M., 2004, XMM-SOC-CAL-TN-0050 (available at: `http://xmm2.esac.esa.int/docs/documents/CAL-TN-0050-1-1.ps.gz`)

Smith M., et al., 2014, XMM-CCF-REL-309 (available at: `http://xmm2.esac.esa.int/docs/documents/CAL-SRN-0309-1-0.ps.gz`)